



Confirmation of sublunarean voids and thin layering in mare deposits

M.S. Robinson^{a,*}, J.W. Ashley^a, A.K. Boyd^a, R.V. Wagner^a, E.J. Speyerer^a, B. Ray Hawke^b,
H. Hiesinger^{c,d}, C.H. van der Bogert^c

^a School of Earth and Space Exploration, Arizona State University, Tempe, AZ, USA

^b Hawaii Institute of Geophysics and Planetology, School of Ocean and Earth Science and Technology, University of Hawaii, Honolulu, HI, USA

^c Institut für Planetologie, Westfälische Wilhelms-Universität, Münster, Germany

^d Brown University, Providence, RI, USA

ARTICLE INFO

Article history:

Received 6 February 2012

Received in revised form

16 May 2012

Accepted 16 May 2012

Available online 26 May 2012

Keywords:

Moon

Volcanism

Impact melt

Shelter

Pit

Flow

ABSTRACT

Typical flow thicknesses of lunar mare basalts were not well constrained in the past, because as craters and rilles age, downslope movement of loose material tends to mix and bury stratigraphy, obscuring the three dimensional nature of the maria. New Lunar Reconnaissance Orbiter Camera high resolution images unambiguously reveal thicknesses of mare basalt layers exposed in impact craters, rilles, and steep-walled pits. Pits up to one hundred meters deep present relatively unmodified, near-vertical sections of mare in three cases, and many young impact craters also expose well preserved sections of mare. Oblique views of each pit and many of these craters reveal multiple layers, 3 to 14 m thick, indicating that eruptions typically produced a series of ~10 m thick flows (or flow lobes) rather than flows many tens to hundreds of meters thick. Additionally, these images unambiguously show that the floors of two pits extend beneath the mare surfaces, thus revealing sublunarean voids of unknown lateral extent. We also document the occurrence of pits that may be expressions of collapse into subsurface voids in non-mare impact melt deposits. These voids are compelling targets for future human and robotic exploration, with potential as temporary shelters, habitations, or geologic museums.

© 2012 Elsevier Ltd. All rights reserved.

1. Introduction

The existence of sublunarean voids was hypothesized as far back as 1885 (e.g., Nasmyth and Carpenter, 1885; Coggins and Pratt, 1952; Halliday, 1966; Heacock et al., 1966; Hatheway and Herring, 1970; Hörz, 1985; Coombs and Hawke, 1992). After the discovery and quantification of the radiation environment in cis-lunar space (Hörz, 1985), it was realized that geologic features such as locally collapsed lava tubes (skylights) could provide access to shelters from radiation and other surface hazards (Hörz, 1985; Coombs and Hawke, 1992; De Angelis et al., 2002). The first steep-walled lunar pits were identified in SELENOlogical and ENGINEERING Explorer (SELENE) Terrain Camera (TC) images (Haruyama et al., 2009, 2010) (Appendix A). The first-discovered pit is located (Fig. 1) in the Marius Hills region of Oceanus Procellarum (14.1°N, 303.2°E) (Haruyama et al., 2009). The two other pits were found within Mare Tranquillitatis (8.3°N, 33.2°E) and Mare Ingenii (36.0°S, 166.1°E) (Haruyama et al., 2010). More than 150 additional pits, of various shapes and sizes, are identified in Lunar Reconnaissance Orbiter Camera (LROC) Narrow

Angle Camera (NAC) (Robinson et al., 2010) images associated with impact melt deposits within 21 craters.

1.1. Terminology

The term ‘pit crater’ can refer to several types of landforms with different formation mechanisms, terrestrial pit craters are typically characterized by circular to oblate outlines, near-vertical walls, a lack of overflow or ejecta on their rims, and an association with volcanic deposits and processes (e.g., Carr and Greeley, 1980; Okubo and Martel, 1998; Howard, 2010). On Earth, pit crater environments include collapsed roofs of small magma chambers or broad cavities, partially drained dikes, and piston-like ground subsidence areas over rift zone fractures (e.g., Carr and Greeley, 1980). Terrestrial pit craters are usually defined as the surface expression of stoping through ceilings of underlying void spaces with eventual surface collapse (Okubo and Martel, 1998; Howard, 2010).

The morphologic characteristics of the three largest steep-walled lunar pits described here are consistent with the terrestrial examples mentioned above. However, enough confusion persists over the precise definition of the term ‘pit crater’ to avoid its use when describing pits that may be lava tube skylights (e.g., Cushing et al., 2007; Halliday 1998, 2008). Though exceptions have been noted, the genetic similarity between lava tube

* Corresponding author. Tel.: +1 4807279691.

E-mail address: mrobinson@asu.edu (M.S. Robinson).

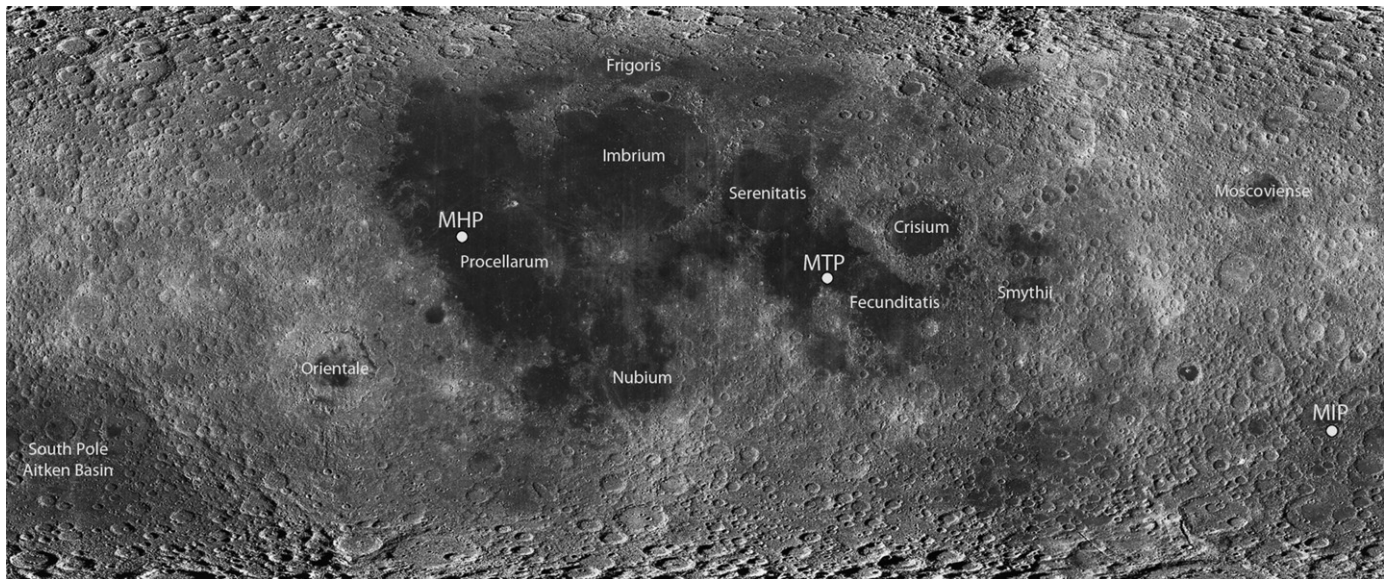


Fig. 1. LROC WAC mosaic showing locations of the three steep walled mare pits, area covers 180 °W to 180 °E longitude, and $\pm 75^\circ$ latitude. MHP Marius Hills Pit (14.091 °N, 303.223 °E), MTP Mare Tranquillitatis Pit (8.335 °N, 33.222 °E), MIP Mare Ingenii Pit (35.950 °S; 166.057 °E).

Table 1

Feature dimensions with LROC derived coordinates.

Feature region (mare or melt pond)	Diameter (m)	Depth* (m)	Location	
			Lat	Long
Ingenii	103, 66	37–63	35.950 °S	166.057 °E
Tranquillitatis	99, 84	107	8.335 °N	33.222 °E
Marius Hills	57, 48	45	14.091 °N	303.233 °E
King pond bridge	56, 24	11	6.241 °N	119.735 °E
Copernicus pond pit	90, 50	23	10.329 °N	339.619 °E

Note: Pit diameters are presented as maximum and minimum.

* Presented depths were measured from the sharp break in slope to the pit floor. Depths are calculated from shadow measurements.

skylights and classic magma chamber pit craters is described as ‘limited’ (Halliday, 1998), with this author calling for a redefinition of pit crater that precludes its confusion with skylights.

Moreover, while the Marius Hills pit is plausibly proposed to be a skylight based on its location within a sinuous rille (Haruyama et al., 2009), less certainty exists for the origin of the Tranquillitatis and Ingenii pits, both located in relative isolation from obvious rille systems. Tectonic features are common in the maria and may play a direct or indirect role in pit formation. Imaging of cavernous interiors extending under a mare (or direct exploration by a landed element) would certainly clarify the origin of the main pit features discussed below. However, until more is known about the formation mechanisms of these mare pits, we adopt the term ‘steep walled pit’, or simply ‘pit’ for brevity.

2. Pit morphology

The NAC images allow detailed topographic and morphologic descriptions of the three mare pits (Fig. 1), giving insight to their origin and significance (Table 1, Appendix A). In the following sections each pit and its local environment are described.

2.1. Mare Ingenii pit

Mare Ingenii embays Thomson (115 km diameter), Thomson M (110 km diameter) and the surrounds, and is one of the larger

farside mare deposits. Mare Ingenii is perhaps most notable for the distinctive swirl patterns that superpose its surface (Hood et al., 1979, Blewett et al., 2011, Kramer et al., 2011). The Ingenii pit is near the center of the crater Thomson M, ~ 10 km west of a knobby region, indicating the mare may be thin in this area. Close to the pit are no distinguishing tectonic or mare flow features: the immediate surrounding mare surface is most notable for their lack of distinguishing features.

The Mare Ingenii pit was imaged by the NAC 13 times with incidence angles (intersection of solar vector measured from the surface normal) ranging from 35° to 82° (Fig. 2). The pit has an ovoid outline with a long axis aligned approximately north–northeast to south–southwest (Fig. 3). Measured from the sharp break in slope along the perimeter, maximum and minimum pit diameters are 104 m and 71 m. Depths from shadow measurements range from ~ 64 m at the south–southwest end to ~ 39 m at the north–northeast end (these measurements are from where the shadow is cast, which is below the level of the surrounding mare). The variable depths result from a sloping talus field that covers much of the pit floor, which may also partially (or completely) obstruct any potential cavern entrance. Depths from shadow estimates are point measurements by nature, and may not fully capture the range of depths from the rim, or fully describe floor roughness. Additionally, a shadow measurement represents depth from the point where the pit slope exceeds the complement of the incidence angle, which is below the level of the surrounding mare surface (there is a shallow, sloping apron surrounding each pit). Depths measured with stereogrammetric techniques (Tran et al., 2010) (M123485893R, M138819477R) range from ~ 38 to ~ 67 m in the same points as the shadow measurements (measured from the lip below the surrounding plain confirming the shadow measurements). The maximum depth below the surrounding mare to the pit floor is ~ 87 m. The pit walls exhibit five measureable layers; from top to bottom their thicknesses are 5, 6, 7, 11, and 8 ± 1 m, respectively. We assume that talus covers the bottom of each layer and does not hide thinner layers.

Block diameters on the pit floor range from 1 m (the smallest detectable size) to 5 m, with the largest fragments clustered at the west (M128202846L) and southwest (M123485893R) ends of the floor. The standard deviation of reflectance values of the west–southwest floor is seven times that of the surrounding mare

Download English Version:

<https://daneshyari.com/en/article/1781451>

Download Persian Version:

<https://daneshyari.com/article/1781451>

[Daneshyari.com](https://daneshyari.com)